UNIVERSIDAD NACIONAL DE COLOMBIA
SEDE BOGOTÁ
FACULTAD DE CIENCIAS
DEPARTAMENTO DE GEOCIENCIAS
RESEARCH GROUP IN GEOPHYSICS

EARTH SCIENCES
RESEARCH JOURNAL

Earth Sci. Res. SJ. Vol. 16, No. 1 (June, 2012): 41 - 53

PETROLOGY

Natural zeolites filling amygdales and veins in basalts from the British Tertiary Igneous Province on the Isle of Skye, Scotland

Juan Manuel Triana R.[1], Javier Francisco Herrera R.[1], Carlos Alberto Ríos R.[1*], Oscar Mauricio Castellanos A.[2], José Antonio Henao M.[3], Craig D. Williams[4] and Clive L. Roberts[4]

[1*] Escuela de Geología, Universidad Industrial de Santander, Bucaramanga, Colombia.
[2] Programa de Geología, Universidad de Pamplona, Colombia
[3] Grupo de Investigación en Química Estructural (GIQUE), Escuela de Química - Universidad Industrial de Santander
[4] School of Applied Sciences, University of Wolverhampton, England
[*] Corresponding author. E-mail: carios@uis.edu.co

ABSTRACT

Natural zeolites filling amygdales and veins in tertiary basaltic host rocks on the Isle of Skye (NW Scotland) have been studied in some detail by transmitted light microscopy, scanning electron microscopy and X-ray diffraction techniques. The zeolites and associated minerals so identified in order of their relative time of formation from early to late were nontronite, amorphous silica phases, carbonate phases, chabazite, phillipsite, wairakite, thomsonite, analcime, natrolite and stilbite-type minerals. Zeolite formation in the Skye basalts began with low Si/Al ratio Na zeolites and a gradual increase in Ca content and Si/Al ratio, ending up as Ca zeolites. They were probably formed as a consequence of late-stage hydrothermal activity, although, locally, contact metamorphism may control the process of zeolite formation.

Keywords: natural zeolite, amygdale, vein, basaltic rock, Isle of Skye.

RESUMEN

Las zeolitas naturales como relleno en amígdalas y venas que ocurren en rocas basálticas Terciarias de la Isla de Skye (NW Escocia) han sido estudiadas en detalle por técnicas de microscopía de luz transmitida, microscopía electrónica de barrido y difracción de rayos X. Las zeolitas y los minerales asociados identificados, en orden de su tiempo relativo de formación, son nontronita, fases de sílice amorfa, carbonatos, chabazita, filipsita, wairakita, thomsonita, analcima, natrolita y minerales tipo estilbita. La formación de zeolitas en los basaltos de Skye comenzó con una zeolita rica en Na de baja relación Si/Al y con el aumento gradual en el contenido de Ca y Si/Al, terminó con una zeolita rica en Ca. Estas probablemente se formaron como consecuencia de una actividad hidrotermal tardía, aunque localmente un metamorfismo de contacto pudo controlar el proceso de formación de las zeolitas.

Palabras claves: zeolita natural, amígdala, vena, roca basáltica, Isla de Skye.

Record

Manuscript received: 16/12/2011
Accepted for publications: 25/05/2012

Introduction

Zeolites are formed during aqueous fluids reaction with rocks in a variety of geological environments (Breck, 1974; Gottardi and Galli, 1985; Weisenberger, 2009). Most zeolite became formed during diagenetic processes in sedimentary rocks (including volcaniclastic deposits) which can be grouped into several geological environments or hydrological systems (Hay and Sheppard, 2001), such as hydrologically open systems (Hay and Sheppard, 2001), hydrologically closed systems (Langella *et al.*, 2001), soil and surficial deposits (Ming and Mumpton, 1989), deep marine sediments (Boles and Coombs, 1977) and marine sediments from arc-source terrains (Boles and Coombs, 1977). Zeolites occurring in volcanic lava flow cavities are formed either during lava pile burial metamorphism (Neuhoff *et al.*, 1999), continental basalts' hydrothermal alteration (Walker, 1960) or diagenesis in areas of high heat flow caused by active geothermal systems (Weisenberger and Selbekk, 2008). Zeolites, as products of hydrothermal crystallisation, are generally known from active volcanic rock- associated geothermal systems. Very little work has been published on zeolite occurrences related to late stage pegmatite crystallisation (Orlandi and Scortecci, 1985) in hydrothermal ore veins (Deer *et al.*, 2004) as alteration products along fault planes (Vincent and Ehlig, 1988) and in hydrothermal fractures and veins in granites and gneisses (Weisenberger and Bucher, 2010). Zeolites are crystalline, microporous, hydrated aluminosilicates of alkaline or alkaline earth metals. The framework consists of $[SiO_4]^{4-}$ and $[AlO_4]^{5-}$ tetrahedra, which corner-share to form open structures; such tetrahedra are linked to each other by sharing all of the oxygen to form interconnected cages and channels containing mobile water molecules and alkali and/or alkaline earth cations (Breck, 1974; Barrer, 1978; Gottardi and Galli, 1985; Szoztak, 1998). Zeolites have been widely used as catalysts, adsorbents and ion exchangers in many technical applications due to their exceptional properties (Breck, 1974; Booker *et al.*, 1996; Dixit and Prasada, 1998; Misaelides, 2011; Loiola *et al.*, 2012). They have become worthy of being called the mineral of the future several countries around the world have made significant progress in the exploring and exploiting of this mineral. However, only a few of the natural zeolites in the world are found in sufficient quantities and having the purity required by industry. The U.S. Geological Survey has reported natural zeolites' worldwide occurrence in the USA, Japan, Korea, Bulgaria, Czechoslovakia, Romania, Hungary, Russia, Yugoslavia, South Africa, Italy, Germany, Turkey and China, the latter having the greatest worldwide production. Clinoptilolite, mordenite, heulandite, chabazite, phillipsite and laumontite are some of the more than 40 known natural zeolites occurring in reasonably high quantities and purity. This study was aimed at recognising natural zeolites filling amygdales and veins in tertiary basaltic host rocks on the Isle of Skye (NW Scotland) for their mineralogical characterisation and determining the sequence of zeolite formation of and that of associated minerals.

Field sampling and analytical methods

A University of Wolverhampton (England) research team was involved in reconnaissance fieldwork on the Isle of Skye (Scotland) during autumn 2008. Fieldwork was primarily focused on localities presenting excellent examples of natural zeolites in spillites from the Skye Main Lava Series (Thompson, 1982; Stuart *et al.*, 2000; Fowler *et al.*, 2004). The sampling strategy consisted of taking samples containing natural zeolites and other secondary minerals filling in amygdales and veins from several outcrops in fresh road cuts and new quarries along the roads. Petrographical and microscopy studies were made of specimens of zeolite-bearing rocks to identify mineral species; this led to clarifying and confirming field observations. A trinocular Nikon (Labophot2-POL) transmitted light microscope was used to observe the minerals' optical properties in thin sections. The mineral phases' morphological features were examined in a scanning electron microscope (ZEISS EVO50), using the following analytical conditions: 1 nA I probe, 20.00 kV EHT, 100 μA beam current, Signal A=SE1, WD=8.0 mm. Natural zeolites' X-ray diffraction (XRD) patterns were recorded with a Rigaku D/max 3B diffractometer operating in Bragg-Brentano geometry with Cu-α1 radiation (λ = 1.5406 Å) at 40 kV and 20 mA and a graphite monochromator. Scan parameters were 0.02° step size, 12 s dwell time and 2–70° 2θ range. The Hanawalt method was used for phase identification using the International Centre for Diffraction Data's (ICDD) crystallographic database powder diffraction file (PDF-2).

Geological setting of the Isle of Skye

The Isle of Skye in Scotland covering 1,656 km^2 is the largest, most northerly island in the Inner Hebrides. It is located on the north-west coast of the Scottish Highlands, bounded on the north by the North Minch (an Atlantic sea channel between the Outer Hebrides islands to the west and the

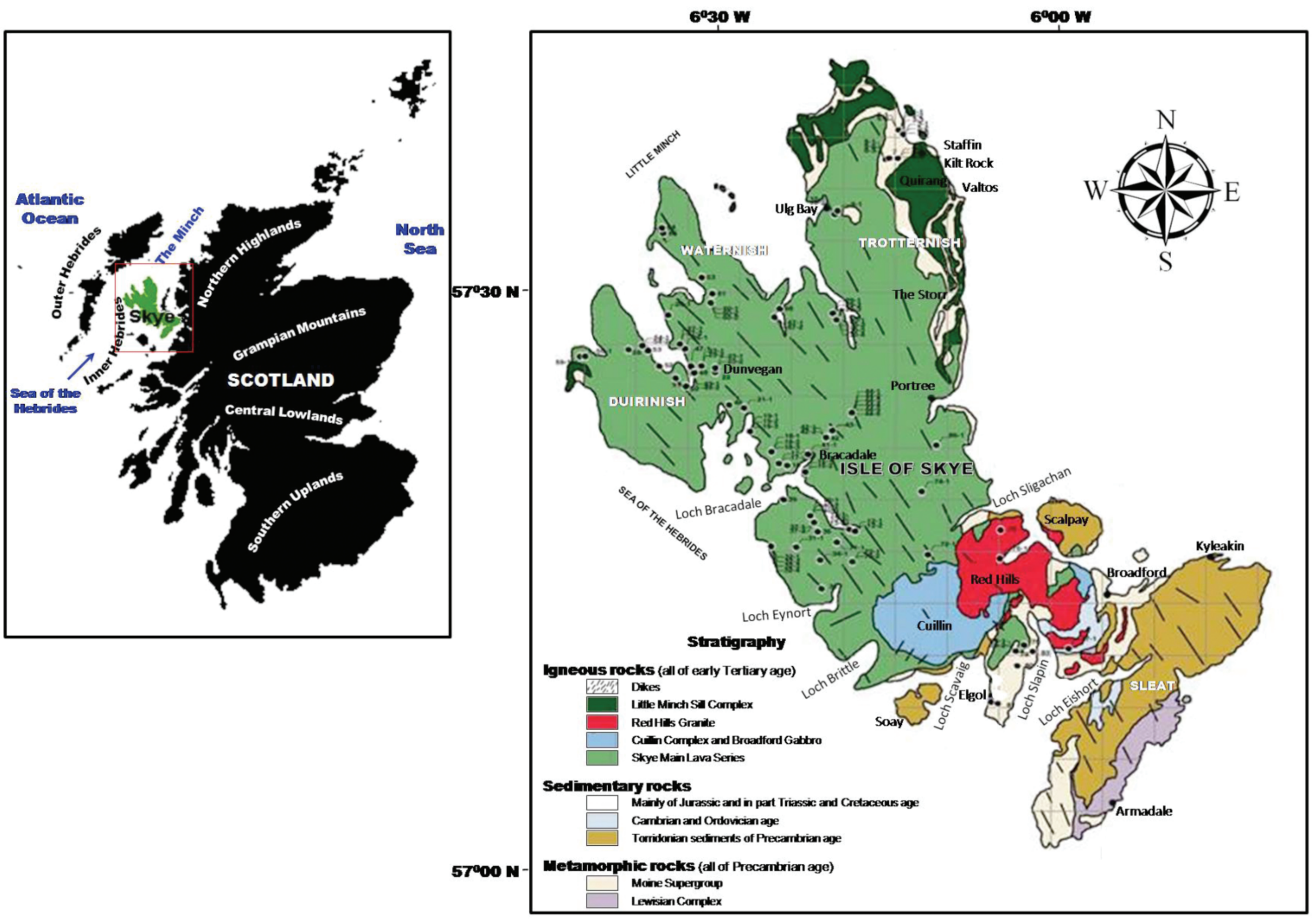

Figure 1. Left, general sketch where the Isle of Skye is located. Right, simplified geological map of the Isle of Skye (adapted and modified from Emeleus and Gyopari, 1992). The sampling sites are indicated by black circles.

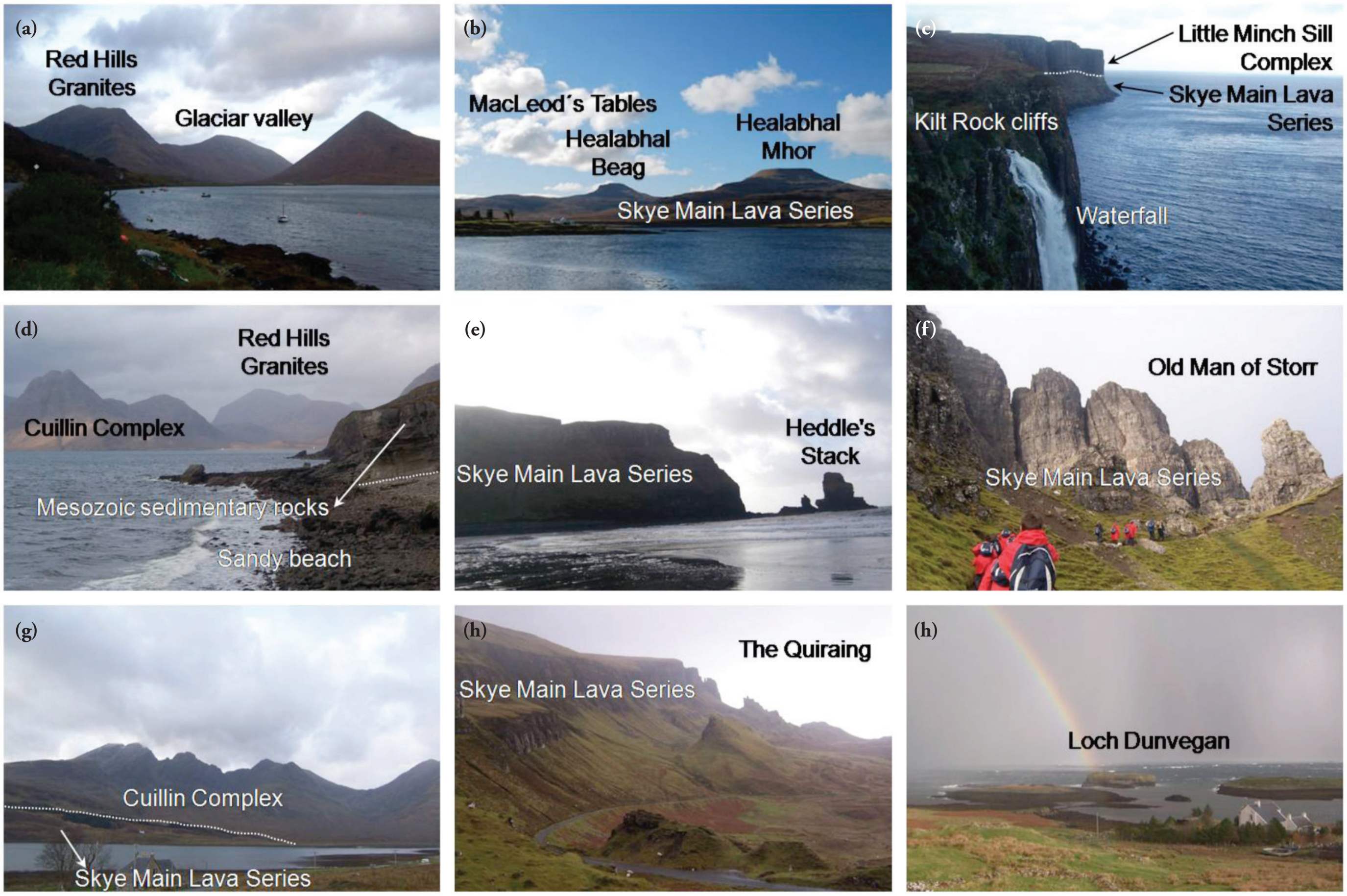

Figure 2. The Isle of Skye's geomorphological features (see text for details).

mainland of Scotland to the east), on the west by the Little Minch (a channel between the Isle of Skye and the outer Hebrides), to the south by the Sea of the Hebrides and to the east by Scotland (Figure 1). The Isle of Skye has a series of peninsulas. Trotternish to the north-east, Sleat to the south-west and Strathraird, Minginish, Duirinish and Waternish to the west. Britain's best ancient landscape is exposed in the Trotternish peninsula. Fractures in the basalt blocks allowed the fall of the main body of lava to slip and rotate on the soft sedimentary rocks below, eventually sliding down the hill to form the Quiraing, Old Man of Storr, the Needle and many other features in a quite particular landscape. Geologically, the Isle of Skye is divided into three provinces: the south-east Sleat Peninsula, the north-west peninsulas and the Red Hills and Cuillin Hills (Figure 1). The oldest rocks (3.000 Ma old Lewisian Complex) on Skye are found on the Sleat Peninsula (Goodenough and Bradwell, 2004). The Lewisian Complex mainly consists of grayish gneiss although it also encompasses quartzites, marbles, graphitic schists and amphibolites, which are thought have been formed from a wide variety of even older igneous and sedimentary rocks whose original composition and structure became modified by the effects of heat and intense pressure deep in the earth's crust (Gibbons and Harris, 1994). Lewisian complex' rocks were caught up during the Caledonian orogeny, and they appear in the hanging walls of the thrust faults formed during the late stages of this tectonic event (Whitehouse and Bridgwater, 2001). These rocks form the basement on which the Moine Supergroup and Torridonian sediments were deposited. The Moine Supergroup consists of a thick and extensive sequence of Neoproterozoic siliciclastic metasedimentary rocks, dominated by psammites with subordinate pelites (Mendum *et al.*, 2008). The complete lack of fossils is consistent with a Precambrian age for the sequence; this is also shown by the age of the earliest known intrusions that cut the sequence, dated at c. 870 Ma. There is also no evidence of the sequence being affected by the 1300-1000 Ma Grenville orogeny (Strachan *et al.*, 2002), suggesting an early Neoproterozoic sedimentation age. Radiometric dating of micas from deformed pegmatites provided the first evidence of a Precambrian metamorphic event of 690-750 Ma (Giletti *et al.*, 1961). The Torridonian sequence describes a series of Neoproterozoic sedimentary rocks, including sandstones, arkoses and shales having coarse conglomerates locally at the base. Radiometric ages from the Torridonian sequence itself give ages ranging from c. 1200-950 Ma (Park *et al.*, 2010). The north-western Duirinish, Waternish and Trotternish peninsulas are composed of Jurassic sediments covered by plateau basalts which erupted from dikes and fissures during the earliest Tertiary time, c. 62 Ma ago (Drury *et al.*, 1976). The latter can be classified as continental flood basalts (CFBs), which appear to have been erupted in a subaerial environment, as indicated by the tectonic environment of continental flood basalt provinces and characteristic continental flood basalt lava flows (Garner, 1996). White and McKenzie (1989) have stated that the eruption of continental flood basalts requires both a mantle source having abnormally high potential temperatures, together with high stretching factors typical of advanced stages of continental extension. Horizontal flows built up on top of each other to a height of around 2,000 ft. The rocks have since been eroded by rivers and ice, leaving flat-capped hills and stepped plateau in the north-west. Spectacular landslides in Trotternish caused by Paleogene age lava falling away from weaker sediments underneath have produced a unique landscape. The spectacular alpine scenery results from the exposed plutons of red granite (Red Hills) having 54±3 Ma Rb-Sr ages (Moorbath and Bell, 1965) and dark gabbro (the Cuillin) intruded 54-62 Ma ago (Ferry *et al.*, 1987). Such intrusions are thus slightly younger than the plateau basalts. These rocks form the highest and most rugged mountain scenery on the island. Gillen (2003) has provided a comprehensive treatment of the geology of the fascinating scenery of Scotland, including the Isle of Skye, having a landscape that has been studied by geologists and geographers from the beginnings of geology as a science. Skye has periglacial cliffs, remote beaches, lakes, irregular rock peaks, steep rocky hills, high peaks and varied geomorphology. Erosion has been the main force in shaping the current landscape, particularly erosion by ice when glaciers covered most of Skye. It highlights the presence of the most rugged mountains in Britain, the imposing Cuillin. More gentle hills are scattered across the island and the long Trotternish summit in the north has a series of landslides on its eastern flank. The coast has steep cliffs caused by weathering (perhaps the most impressive in Britain), sea stacks, caves, arches and waterfalls (Townsend, 2001). Figure 2 illustrates characteristic landforms on the Isle of Skye. Figure 2a shows the typical morphology of a glacial valley at Loch Slapin Bay. Macleod's Tables are two curious flat-topped hills which are prominent in views from many parts of Skye (Figure 2b); they consist of two plateaus, Healabhal Mhor (MacLeod's Plateau North) and Healabhal Bheag (MacLeod' s Plateau South). Figure 2c shows the waterfall at the Kilt Rock which is the geomorphological expression of the Little Minch Sill Complex on the top of the Skye Main Lava Series. The view is of the cliff face to the north which shows good columnar jointing and there are also complete columns which have fallen on to the beach. A typical depositional coastal landform is represented by a sandy beach (Figure 2d). Talisker Bay is one of the most long-standing and best-known sites on the Isle of Skye, partly due to being one of the more accessible of the Skye Main Lava Series and, more importantly, to the bay's sea stack, the Heddle's Stack (Figure 2e). The Old Man of Storr is a slipped rock pinnacle (Figure 2f); the basalt lavas that make up the Old Man and the rock face behind it are clearly in layers representing different lava flows. The Cuillin represents the deeply eroded roots of large volcanoes active some 60 Ma ago (Figure 2g). Sgurr Alasdair is the highest point of the Cuilli hills and the Isle of Skye (3,255 ft). The Quiraing is a landslip on the eastern face of Meall na Suiramach, the northernmost summit of the Trotternish Ridge on the Isle of Skye (Figure 2h). Distinctive features of this landscape include the Needle (a jagged 120 ft high landmark pinnacle), the Table (a flat grassy area slipped down from the summit plateau) and the Prison (a pyramidal rocky peak which can look like a medieval keep when viewed from the right angle). Loch Dunvegan is a sea loch on the west coast of the Isle of Skye (Figure 2i).

Natural zeolite-bearing rocks at the Skye igneous centre

The Skye igneous centre forms part of the British Tertiary Igneous Province manifest as a series of voluminous mafic to silicic magmatism in mainland western Scotland and the offshore Hebridean islands associated with the opening of the North Atlantic Ocean (Saunders *et al.*, 1997). The plutonic complexes and associated lava fields were produced between 58 and 62 Ma ago (Hamilton *et al.*, 1998). The igneous rocks exposed on the Isle of Skye represent the eroded remains of one of the major igneous centres along the western shore of Scotland. Stuart *et al.*, (2000) have described the Tertiary igneous rocks on the Isle of Skye in detail, including the following units: Little Minch Sill Complex, Skye Main Lava Series, Red Hills Granites and Cuillin Complex and Broadford Gabbro. The Little Minch Sill Complex became emplaced into Middle Jurassic sediments underlying the Skye Main Lava Series, although intrusive relationships suggest that it is marginally younger than the lavas (Gibson, 1990). Gibson and Jones (1991) have stated that is composed of both single and multiple sills, represented by three main, genetically related units: picrite, picrodolerite and crinanite (analcime-rich dolerite); these are the result of the differentiation of an alkali-olivine basalt magma in an upper-crustal magma chamber. The eastern side of Trotternish Peninsula is characterised by a series of dolerite sills; the best known being the Kilt Rock. The Skye Main Lava Series crops out in north and west-central Skye, covering 1500 km^2 (over 1200 m and with a cumulative thickness). Each lava field's stratigraphy has been established by using deep weathering profiles and fluvial to lacustrine sedimentary intercalations which developed during hiatuses in volcanism (Thompson, 1982). These rocks predominantly consist of transitional to alkaline and tholeiitic lava flows on top of the sequence erupted c. 58 Ma ago (Bell and Jolley, 1997; Hamilton *et al.*, 1998). The importance of the town of Portree is its exposure through the Beinn Edra Group which forms the basis of the Skye Main Lava Series (Emeleus and Gyopari, 1992). At least 24 lava flows have been recognised by Anderson and Dunham (1966), which accumulated after being subjected to deep weathering in wet, warm tropical or subtropical conditions (Emeleus and Gyopari, 1992). A central intrusive complex having four major centres of activity represented by multiple intrusions developed in succession as the focus of igneous activity moved progressively eastward at the end of the period of flood basalt volcanism (Fowler *et al.*, 2004). From west to east, these are the Cuillin centre, the Srath na Creitheach centre, and the Western and Eastern Red Hills centres (Bell, 1976; Emeleus and Gyopari, 1992). The Cuillin centre is a composite confluent intrusion ranging in composition from peridotite to gabbro (Stuart *et al.*, 2000). Although they post-date most basalts, the Cuillin intrusive complex is most likely coeval with the latest Skye Main Lava Series tholeiitic basalt flows. Dickin and Exley (1981) reported an age of 59.3±0.07 Ma for the youngest Cuillin centre intrusion, the Coire Uaigneich Granophyre. The Srath na Creitheach centre is small and poorly documented and consists of volcaniclastic breccias, post-dating the Cuillin centre but pre-dating the Red Hills granites (Trewin, 2003). The southern part of the Isle of Skye is dominated by the Red Hills alkali granites. Age determinations have been reported as 58.7±0,9 Ma for the Loch Ainort granite (Western Red Hills centre) and 53.5±0,9 Ma for the Beinn an Dubhaich granite (Eastern Red Hills centre) (Dickin, 1981). The presence of hybrid bodies in the Western and Eastern Red Hills centres suggests that basaltic magma was available during granitic centre formation (Fowler *et al.*, 2004). Further evidence of this is the intrusion of mafic to intermediate cone sheets and dykes throughout the history of the central complex, which are coeval with many of the above Cuillin rocks (Emeleus and Gyopari, 1992). According to Emeleus and Gyopari (1992), the Cuillin centre's gabbros and peridotites were cut by numerous basaltic cone-sheets and subsequently by Red Hills' granites. The central complexes thus record varied intrusive sequences in which basaltic and granitic magmas have been intimately associated.

Field occurrence of natural zeolites in spillites from the Skye Main Lava Series

The occurrence of different zeolites and other secondary minerals from the Skye Main Lava Series and their frequency are not homogeneous and their spatial distribution is directly controlled by host rock's chemical composition and local hydrothermal conditions (Weisenberger and Spürgin, 2009). Host rock porosity controls the fluid/rock interaction. Descriptions of zeolite appearance, occurrence and textural relationships are given below. Some very small amounts of zeolite-like species still require further investigation regarding their characterisation. Outcrops containing zeolites mostly correspond to transitional to alkaline basalts differing in colour, degree of weathering and content and distribution of amygdales and veins now filled with zeolites. Spillitic basalts (making up most outcrops) are dark gray with zeolites developed in randomly arranged veins and cavities. A zeolite occurrence was found in a basalt quarry near Dunvegan where zeolites occur in scarce, elongated amygdales having considerable sizes up to 10 cm (Figure 3a) hosted by columnar basalts usually showing a red-brown weathering surface (Figure 3b), as observed in the small village of Dunans. Gray spillitic basalts with zeolites developed in irregularly shaped cavities in contact with a floor of red laterite overlain by highly vesicular basalts without zeolites having a light brown weathering surface occur in the same village (Figure 3c). The red laterite is formed by the deep weath-

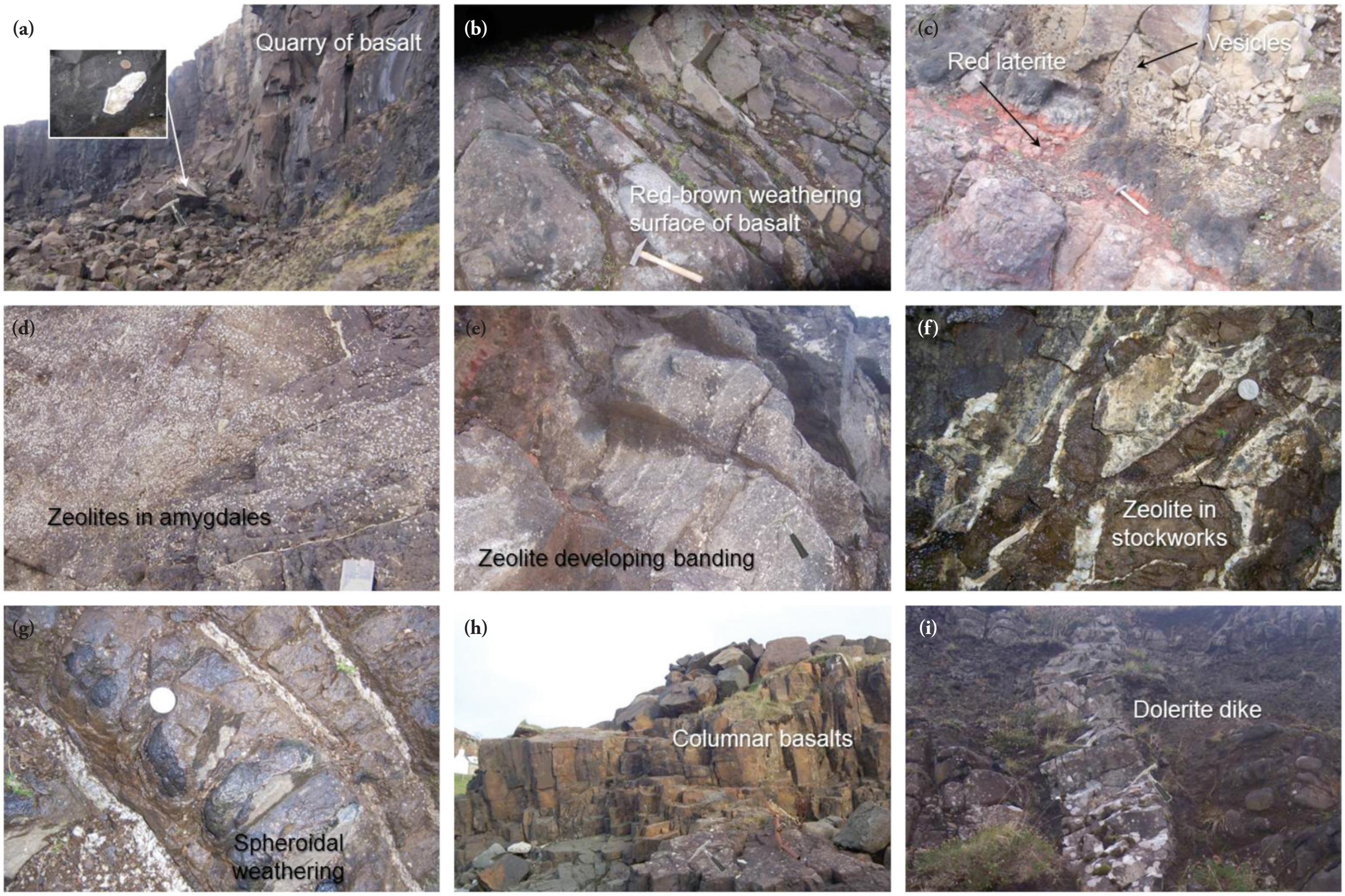

Figure 3. Outcrop-scale features illustrating the occurrence of zeolite-bearing basalts and associated rocks from the Skye Main Lava Series (see text for details).

ering of the upper layers of lava flows before the next one had erupted. In some cases, contact between spillitic lava flows marks a contrast in the degree of weathering, colour and development of layering, reddish-brown meaning a greater degree of weathering and vesicular random distribution, which apparently contain a smaller amount of zeolite amygdales. A typical example of zeolite occurrence in amygdales can be observed at Talisker Point (Figure 3d). The degree of these dark gray spillitic basalts' weathering is low near the Quiraing, eventually reaching cavities containing zeolites to become concentrated so that they develop a banding (Figure 3e). Zeolites occur in veins at Treaslane, a small remote scattered crofting hamlet overlooking the western entrance to Loch Treaslane; they may be parallel or develop stockworks (Figure 3f). Sometimes massive green basalts outcrop in contact with highly weathered gray to red spillitic basalts having spheroidal weathering can be observed near the Quiraing (Figure 3g). One of these contacts in particular shows a dolerite sill along the plane of contact. Veins containing zeolite material appear in some surfaces of spillitic basalts parallel to the lava flow (up to 3 cm thickness) or transverse to it in several directions. When there are many veins they develop as stockworks (rock masses very interpenetrated by small veins) which, in some sectors, have a brecciated appearance. Veins thickness is not uniform. The veins described above are present in basalts having spheroidal weathering, produced through perpendicular joint systems. Columnar basalts falling right to the sea in horizontal rock formations resulting from the lava flows' rapid cooling may be observed at Allt Luig Mhóir (Figure 3h). Locally, dolerite dikes cutting spillitic basalts appear smaller and are easily visible at Allt Coir' a Ghabhainn (Figure 3i). No discernible chilling is seen towards their margins, but the presence of zeolite-filled cavities (amygdales) is common in a number of the dykes (Bell, 1984).

Petrographical analysis

Figure 4 shows zeolite's general macroscopic characteristics, as seen in the field. Zeolites appear filling cavities in a non-uniform way; sometimes they just line cavities and sometimes they fill them completely. They are associated with other secondary minerals such as amorphous silica, calcite and nontronite. Amygdales have a spheroid, ellipsoidal or irregular shape; they usually appear in separate units but locally coalesce with each other (Figures 4a-4b). They are usually about 0.5-1.5 cm in diameter but could locally reach up to 10 cm. Drusy amygdales, having a partial filling, may exhibit various types of zeolite material, a certain amount of crystals having well-defined faces in the centre of the cavity and massive granular aggregates with vitreous luster covering the walls of the cavity (Figures 4c-4f). A combination of irregular and large amygdales ranging from 1.0 mm to 1.0 cm and having a massive appearance contrasts with vesicles lacking any kind of padding. Radial aggregates of zeolites with vitreous luster usually occur in irregular amygdales of variable shape and size, some up to 5.0 mm in diameter being semi-spherical and others up to 1.2 cm being spherical (Figures 4g-4h). Zeolites also occur in fibrous aggregates, partly or completely filling spheroid, ellipsoidal or irregular amygdales (Figure 4i). Irregular to ellipsoidal shaped amygdales (up to 2.0 cm) may be completely filled by crystals, revealing the occurrence of at least two zones: a fibrous lining in the outer part of the cavity wall and a fibrous interior padding. Moreover, amygdales whether spheroid, elongated or irregular shaped may have a well-defined layer of fibrous material that only occurs in the outer part of the cavity wall. In some cases, a zoning zeolite distribution can be distinguished; fibrous zeolite phases displaying a silky luster in the outer part of the cavity wall and granular zeolite phases having a glassy

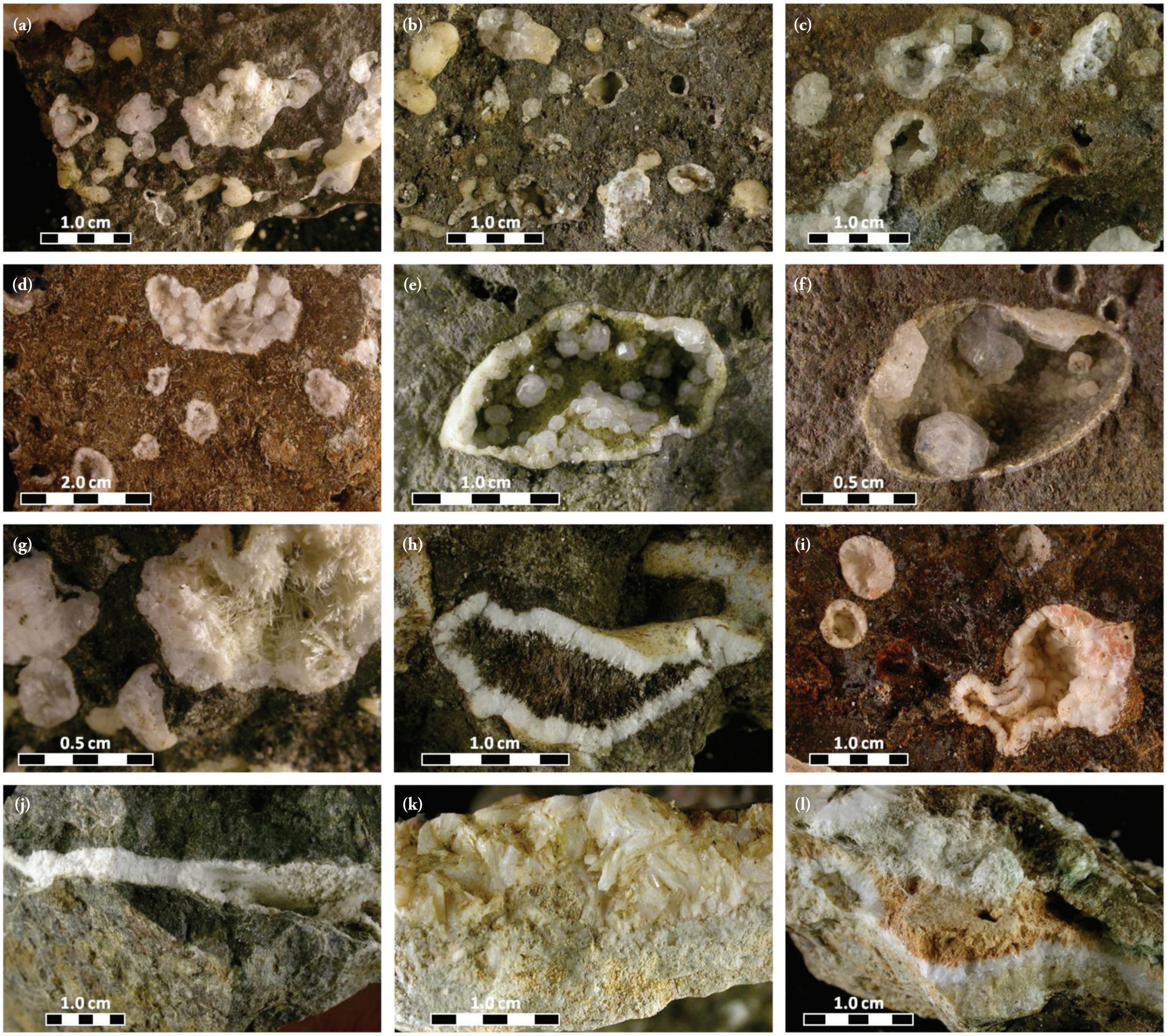

Figure 4. Macroscopic scale features illustrating the occurrence of several types of zeolites in amygdales and veins (see text for details).

luster as an interior padding. A different zeolite occurrence can be observed in veins traversing basalts; these veins are up to several centimetres thick and can be as much as a few meters long. Zeolites are white with silky luster and show a predominance of fibrous aggregates although these can intergrow with acicular and radial aggregates (Figures 4j-4l). It is sometimes difficult to identify the type of aggregate due to the diversity of varyingly shaped and sized minerals. Cross-linked aggregates intergrown with tabular aggregates can be distinguished in some veins, whereas only tabular, radiated and yellowish-white aggregates can be recognized in others. Most zeolites are relatively coarse-grained and easily identifiable. However, they sometimes occur as fine-grained aggregates, which are very difficult to identify. Zeolytic phases and associated secondary minerals in basalts were sequentially deposited from the outer wall to the centre of amygdales and veins. Chabazite is usually vitreous and colourless to pink. It is cubic to rhombohedral. However, other more complex forms also occur, mainly developing regularly twinned crystal intergrowths. Phillipsite is uncommon and is normally the sole occupant of vesicles. Wairakite is generally vitreous with well-formed pseudo-octahedral to pseudo-icositetrahedral colourless crystals which can be confused with analcime. Thomsonite varies in habit showing bladed crystals, spherulites, radial crystal groups and rich coatings mainly made up of small crystals, although it sometimes has a fibrous nature. Analcime appears as vitreous and granular well-formed trapezohedral crystals which are often colourless and sometimes white. Natrolite is generally beige to white, either massive or forming radiating fibres and shows a more glassy brightness than mesolite, which is generally milky white and fibrous, having larger fibres than those of natrolite. Stilbite commonly occurs as vitreous sheaves or plates, ranging from colourless to green to white.

Figure 5 illustrates the main microscopic features of the zeolites investigated here and associated mineral phases. The vesicles and fractures in basalts were gradually filled up with secondary minerals, developing amygdales and veins usually showing mineral zoning distribution though, in some cases, they were not completely filled. Figure 5a gives an example of the occurrence of a mixed layer of celadonite (Fe-rich mica) and nontronite (Fe-rich smectite) and vesicles commonly lined by these mineral phases. Celadonite is usually green and botroidal and has fibrous sphe-

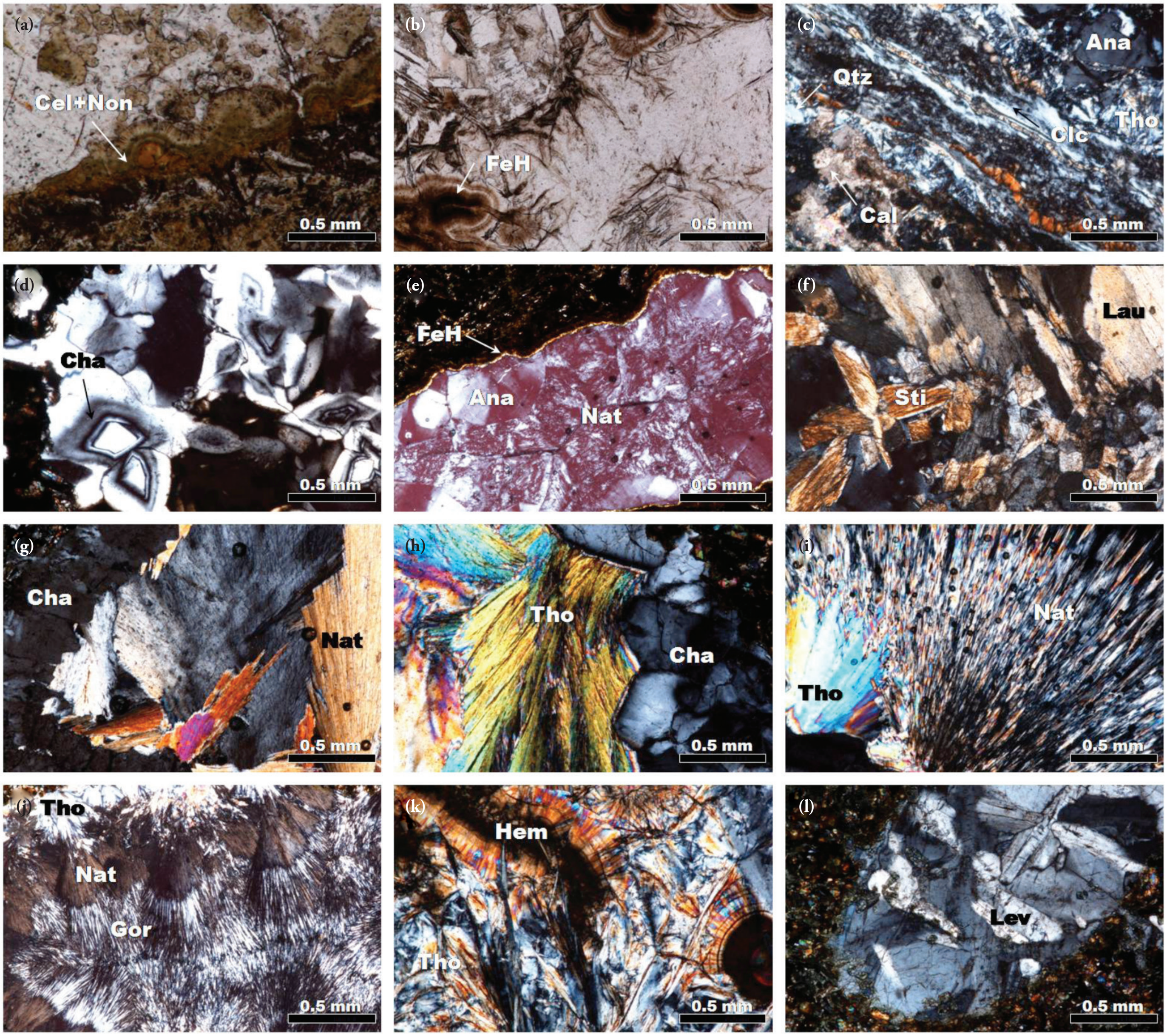

Figure 5. Cross-polarised light (XPL) photomicrographs of the occurrence of several types of zeolites in amygdales and veins (see text for details).

roidal morphology, having detectable striated birefringence under crossed nicols. Nontronite is typically brown in transmitted light and does not have a discernable structure except for banding parallel to the cavity wall. It occasionally exhibits geopetal features. The vesicles are sometimes lined by Fe-oxyhydroxides (Figure 5b), displaying similar morphology to that described for the celadonite-nontronite mixed layer. Figure 5c shows a composite vein characterized by the occurrence of analcime- and thomsonite-associated quartz and calcite. Chalcedony shows a banded structure, consisting of innumerable cryptocrystalline silica grains. It occurs as parallel fibres or in radial or spherulytic aggregates. Chabazite shows a typical rhombohedral habit, sometimes having angles about 90° between their faces. It is colourless and presents dark-grey almost black interference colours and symmetrical extinction (Figure 5d). Analcime occurs as white trapezohedral crystals, low birrefringence, optical zoning and penetration twinning, and it sometimes occurs along with fibrous natrolite radial aggregates (Figure 5e). Figure 5f shows an intergrowth between large laumontite crystals and twinned stilbite crystals. Laumontite was determined taking into account the following optical properties: prismatic crystals with acute ends and diamond-shaped cross-section, having low relief and low refraction index. Stilbite occurs as idiomorphic, tabular crystals forming sheaf-shaped aggregates. It is colourless and shows interference colours of the middle of the first order. Natrolite associated to chabazite occurs toward the centre of an irregular amygdale (Figure 5g). It develops fan-like aggregates of acicular crystals having a moderate yellowish birefringence. The optical properties making it clearly distinguishable from other zeolites are the extinction of the fibres parallel to its length between crossed nicols and the absence of an optical figure in convergent polarised light. Mesolite, scolecite and thomsonite can occur as overgrowths on natrolite. Figure 5h illustrates the association between thomsonite and chabazite. Thomsonite occurs as fibrous radial aggregates, which are colourless in plane polarised light and show first order gray in crossed nicols. Mesolite occurs as long fibrous to acicular crystals grouped in radial aggregates. Scolecite usually occurs as acicular (needle-like) and fibrous aggregates. At least two varieties of fan or radial aggregates of fibrous zeolites occur together as illustrated by Figure 5i (natrolite epitaxial growth on thomsonite) and Figure 5j (natrolite and gonnardite epitaxial growth on thomsonite).

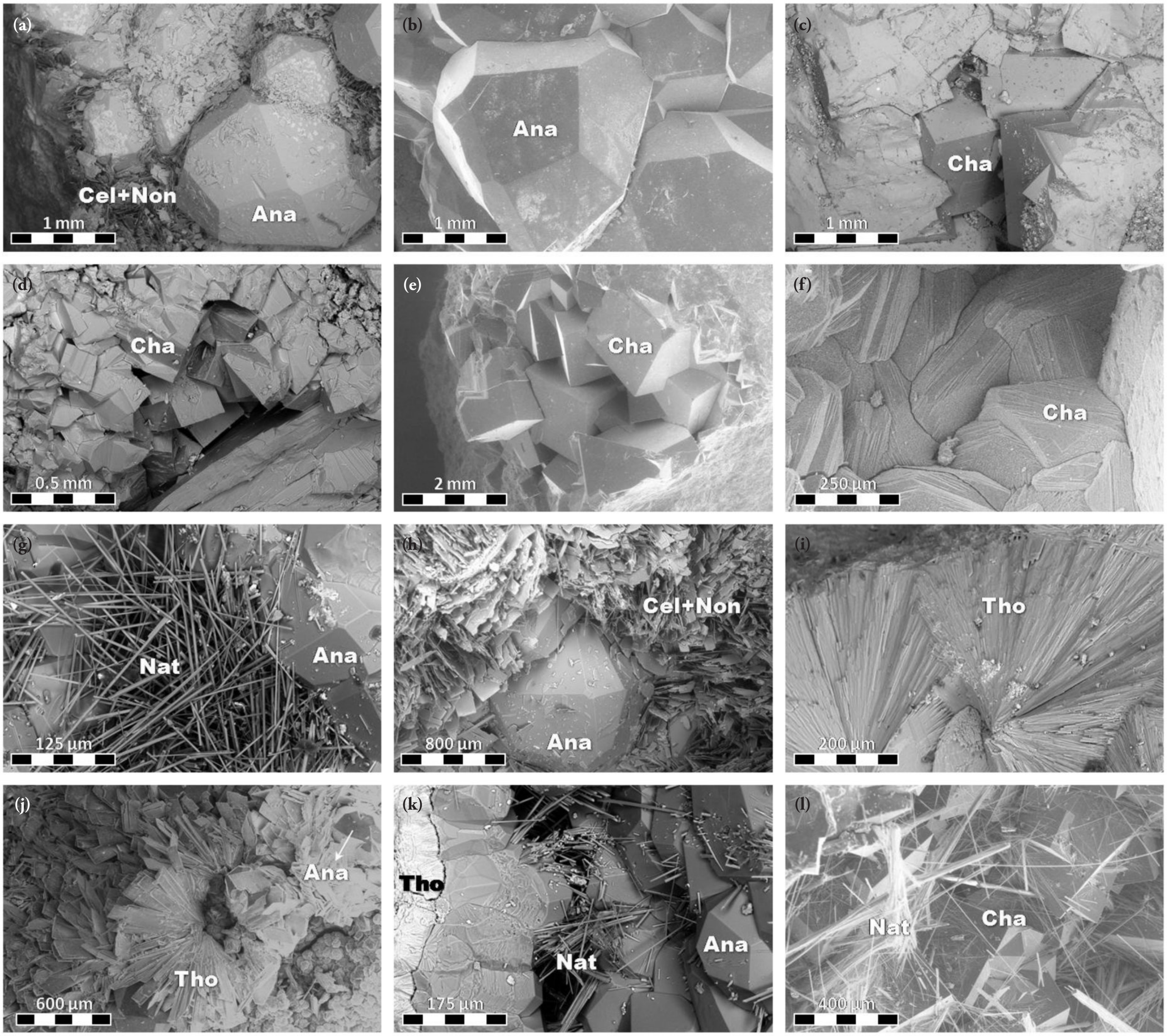

Figure 6. Scanning electron microscope images illustrating morphological features regarding several types of zeolites filling amygdales and veins (see text for details). Ana, analcime; Cha, chabazite; Nat, natrolite; Non, nontronite; Tho, thomsonite.

Figure 5k shows the occurrence of neddle-like crystals of thomsonite along with botroidal and fibrous spheroidal Fe-oxyhydroxides. A fibrous and reticulate aggregate which is transparent to translucent having a variety of colours ranging from white to yellow to reddish gray, can be attributed to levyne (Figure 5l). This zeolite has a moderate relief, low refractive index and is presented as the only infill in certain amygdales.

Scanning electron microscopy

Figure 6 illustrates SEM images of the natural zeolites. Analcime crystals displaying intergrowth and typical isometric morphology (up to 1.8 mm) can be clearly seen in Figures 6a (trapezohedral habit) and 6b (pentagonal dodecahedron habit). The mixed nontronite-celadonite layer appears as tiny plates or flakes by SEM. Chabazite has a variable morphology, reaching up to 800 µm. It usually occurs as rhombohedral crystals developing interpenetration twinning (Figures 6c-6d). In other cases, it has a pseudocubic habit in which angles between their faces are closer to right angles (Figures 6e) Figure 6f gives an example of complexly-twinned (phacolitic) chabazite crystals, showing streaks parallel to the edges of the crystal. Natrolite occurring as groups of randomly oriented acicular crystals associated with trapezohedral analcime crystals is illustrated in Figure 6g. Nontronite occurs as fine-grained random aggregates of flaky crystals along with trapezohedral analcime crystals (Figure 6h). Thomsonite appears as long tabular crystals (up to 1.5 mm in length) arranged in fan-shaped or radial divergent aggregates (can be completely closed taking on a spherical appearance) as shown in Figures 6i and 6j. However, it also occurs as acicular to elongated tabular crystals (up to 650 µm in length) developing radial aggregates. Figure 6k illustrates an example of zeotypes' spatial distribution in amygdules, thomsonite displaying the typical radial fibrous aggregates in the other part of the cavity wall, followed by natrolite occurring as fine fibres forming clusters sometimes growing on typical trapezohedral analcime crystals growing in the centre of the cavity. Needle-like and pointed natrolite crystals (up to 2 mm in length) are wildly dispersed among pseudocubic chabazite crystals (Figure 6l).

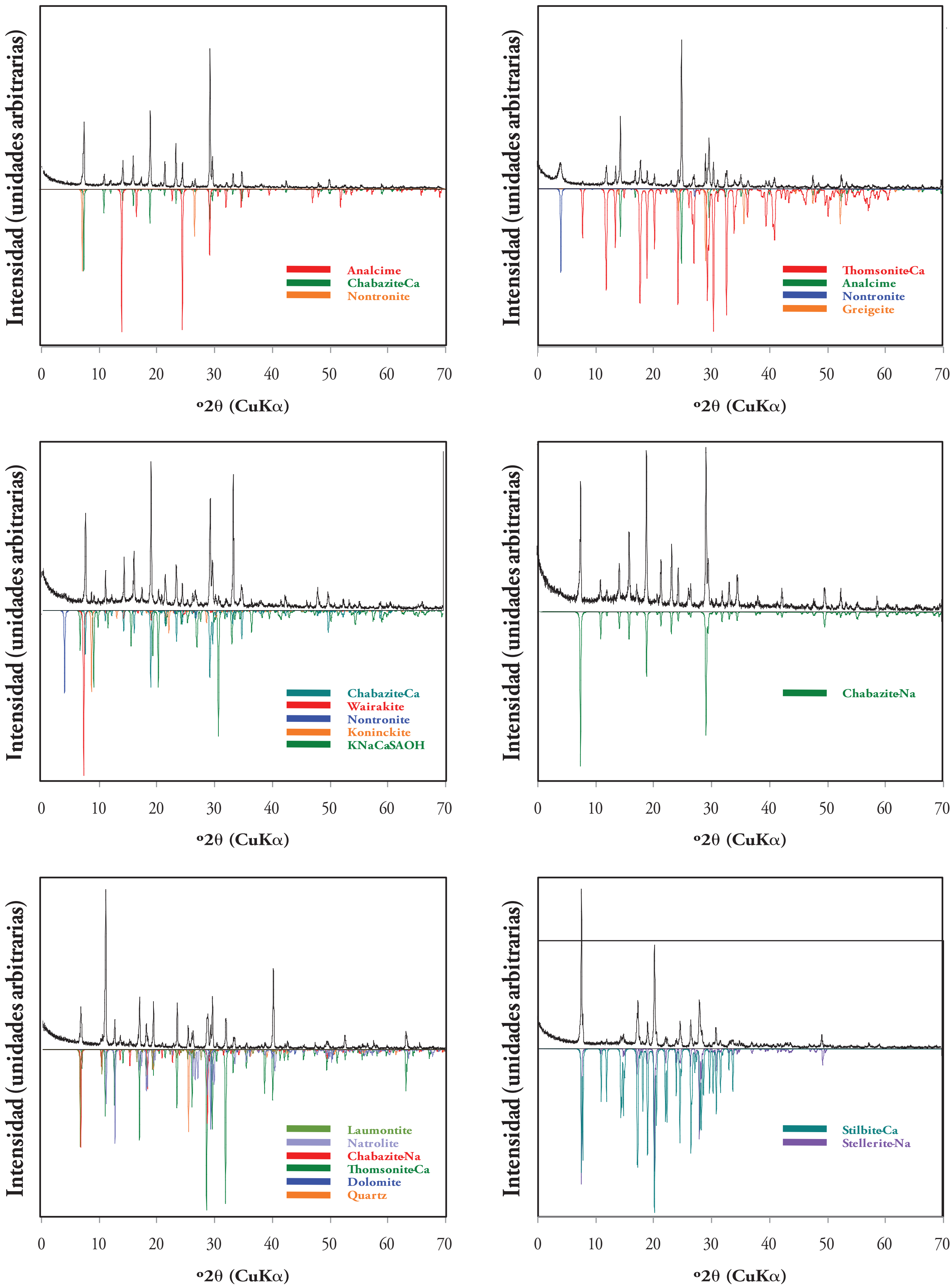

Figure 7. XRD patterns showing the occurrence of zeolites in amygdales and veins (see text for details). KNaCa-SAOH, KNaCa silicon aluminum oxide hydrate.

Table 1. Comparing the zeolite phases identified in this study and the Meier's structural classification (1968).

Structural classification	Identified zeolitic phases
Heulandite group (C4-C4-T1)	stellerite, stilbite, stellerite-Na, Stilbite-Ca
Chabazite group (C6)	chabazite, levyne, chabazite-Ca, chabazite-Na
Analcime group (C4-C4)	analcime, wairakite, analcime-Mg
Natrolite group (C4-T1)	natrolite, thomsonite, thomsonite-Ca
Phillipsite group (C4)	phillipsite, phillipsite-Na
Laumontite group (C8)	laumontite

X-ray diffraction

Qualitative XRD analysis led to identifying a variety of zeolite species, including analcime, as the dominant zeolytic phase, followed by chabazite, natrolite, thomsonite, wairakite, stilbite, stilbite-Ca, phillipsite and stellerite-Na, thomsonite-Ca, chabazite-Ca and chabazite-Na, with minor stellerite, laumontite, levyne, phillipsite-Na, and gyrolite. Other secondary minerals associated with zeolites were celadonite (Fe-rich mica), nontronite (Fe-rich smectite), greigeite (iron sulfide mineral), koninckite or bobierrite (phosphates), alunite (sulphate), truscottite (silicate), calcite or dolomite, and quartz. Nontronite occurred in most samples. Figure 7 illustrates representative zeolites diffraction patterns and associated phases. Figure 7a reveals a typical assemblage of analcime and chabazite-Ca, accompanied by nontronite. The main zeolytic phases shown in Figure 7b are analcime and thomsonite. Other minerals are nontronite and greigeite. The XRD pattern in Figure 7c shows chabazite-Ca occurrence with traces of wairakite, nontronite and koninckite. A characteristic chabazite-Na XRD pattern is illustrated in Figure 7d. Figure 7e reveals the occurrence of thomsonite, chabazite- Na, laumontite and natrolite, along with quartz and dolomite. A stilbite-Ca + stellerite-Na assemblage is illustrated in the XRD pattern shown in Figure 7f. Several zeolytic phases were identified in this study which could be organised into six structural groups according to Meier's classification (1968), as depicted in Table 1. The heulandite group corresponding to the secondary unit C4-C4-T1 was represented by the following zeolites stellerite, stilbite, stellerite-Na and stilbite-Ca. The chabazite group (secondary unit C6) was characterised by the presence of chabazite, levyne, chabazite- Ca and chabazite-Na. The analcime group (secondary unit C4-C4) included analcime and wairakite. The natrolite group (secondary unit C4-T1) was made up of natrolite, thomsonite and thomsonite-Ca. The phillipsite group (secondary unit C4) was represented by phillipsite and phillipsite-Na. The last group consisted of secondary unit C8 with a single zeolytic phase (laumontite). The following associations of zeolytic phases were determined: laumontite + chabazite; wairakite + chabazite; chabazite + thomsonite; analcime + thomsonite; thomsonite + wairakite + chabazite; thomsonite + analcime + chabazite; natrolite + analcime + thomsonite. These mineral assemblages usually showed the additional occurrence of non-zeolite phases such as nontronite and celadonite.

Discussion on zeolite formation

The Isle of Skye is particularly known for its abundance and variety of minerals from the zeolite group and other secondary minerals in tertiary alkali olivine basalts. Their distribution has been controlled by a combination of factors such as temperature, pressure, hot aqueous fluid circulation and rock's chemical composition (Walker, 1960). A study of the Beinn Edra Group lavas by King (1977) revealed the occurrence of similar parageneses of zeolites to those of the analcime-natrolite zone defined by Walker (1960). The zeolites and associated secondary minerals were sequentially deposited from the outer wall to the centre of amygdales and veins in the basalts (Figure 8). Chemical elements necessary for the formation of these mineral phases were released directly as a result of hydrothermal devitrification. However, Ferry *et al.*, (1987), based on oxygen and hydrogen isotope evidence for widespread element exchange between rock and fluid, revealed that basalts from the Skye Main Lava Series were locally affected by contact metamorphism associated with the intrusion of tertiary Cuillin Complex gabbros and Red Hills granites and hydrothermal alteration due to the convection system induced by such intrusions. Zeolites were probably formed from fluids, which penetrated the vesicles and fractures, but the source of the fluid remains unknown. No regional zoning of zeolite assemblages was apparent in this study. Figure 8 shows that the zoning sequence and textural evidence suggest the following crystallisation sequence: first K-rich clay (nontronite) followed by K-rich mica (celadonite), carbonate (calcite), cryptocrystalline silica (e.g. chalcedony), then thomsonite followed by chabazite, analcime, phillipsite and wairakite, and natrolite, laumontite, and stilbite-type minerals (stilbite and stellerite). Zeolites' stability fields are known from modern hydrothermal systems (Kristmannsdóttir and Tómasson, 1978) and the observed sequence in the samples studied here conformed to a progressive decrease in temperature favouring hydrothermal system hydration. The amygdales and veins thus showed a wide range of variability regarding the zeolite minerals present. The irregular zeolite and related mineral distribution in the basalts has been attributed to factors such as localised heat-flow, ionic activity in pore waters and host rock permeability (Pe-Piper, 2000). The high initial permeability subsequently decreased due to secondary mineral deposition, leading to the formation of individual closed systems (Keith and Staples, 1985). Although there is zoning sequence and textural evidence of open-system hydrothermal activity for the formation of the Skye basalt zeolites in amygdales and veins, restricted domains may have developed as pore space became filled by precipitates of mixed-layer nontronite-celadonite, calcite, cryptocrystalline silica and zeolites. The hydrothermal pathways may have been substantially different, even for quite closely spaced cavities. It is probable that a variation in the nature of the exchangeable cations in zeolites occurred within a single amygdale or vein. Fluid composition may be important in defining the type of zeolite that occurs in a particular amygdale or vein, whereas temperature variations may influence chemical variation within such individual cavities. Starting material composition, especially Si/Al ratio, determined the type of zeolite formed (e.g. Boles, 1977). This parameter was most important during the first stages of alteration, in which, usually, an alteration product having a Si/Al ratio similar to or less than that of the starting material became formed. As alteration proceeded, the minerals being formed became poorer in SiO_2, suggesting that hydrothermal desilification took place with continued reaction. The starting material's alkali/calcium ratio may also have influenced the reaction product during early stages of alteration if the reacting solution had a low concentration of these cations.

Si activity in the fluid was low by the time of zeolite crystallisation because it had been used up in chalcedony formation (Chipera and Apps, 2001). The secondary minerals nontronite and locally celadonite represent the first crystallised species lining the outer part of the cavities. Other mineral phases occurring during the early stage were calcite and cryptocrystalline silica. Nontronite was probably formed by basalt devitrification due to hydration, although ferromagnesian mineral phases present in the basalts might have also contributed to its formation. The formation of a Fe-(hydro)oxide celadonite and opaline mixture is thus suggested, which may be explained by silica glass replacement, similar to that reported by Bustillo and Martínez-Frías (2003). High carbonate ion activity caused the early precipitation of calcite, removing most Ca^{2+} ions and so leaving the water comparatively enriched in alkalies. Both celadonite precipitation (which increased the Na+/K+ ratio in solution) and decreased temperature (which favoured Na enrichment in the solution) may have contributed to analcime crystallisation and that of other Na-rich zeolites (Alt and Honnorez, 1984). Thomsonite is the most common zeolite phase formed after nontronite/celadonite. Chabazite, analcime, phillipsite and probably wairakite are the first zeolites which became crystallised. They were followed by acicular-fibrous zeolites such as natrolite/gonnardite, thomsonite, mesolite and scolecite. Analcime is usually a Na-rich mineral phase, but may sometimes contain appreciable K (Utada, 1970). However, this mineral sequence was probably affected by contact metamorphism which could explain analcime formation accompanied by decreasing Si activity and increasing temperature (not reflected in Figure 8). In the SiO_2-deficient environment defined in this study wairakite and analcime may have formed a complete solid solution. Na-rich zeolite precipitation on the wall of amygdales and veins reduced the solution's alkalinity. At lower temperature, Na was accommodated in the structure of chabazite and other zeolites such as analcime and final crystallisation was represented by only small amounts of Na-rich zeolites (natrolite group). Therefore, the existence of nontronite, which is a smectite group low-temperature mineral, along with very well-developed zeolite crystals of analcime, chabazite-Na and probably phillipsite in the edges of cavities, revealed that these mineral phases were deposited prior to fibrous zeolites such as natrolite, being indicative of low-T hydrothermal alteration (<100°C) as stated by Deer *et al.*, (2004). Chipera and Apps (2001) have stated that phillipsite is usually caused by host basalt low-temperature hydrothermal alteration (around 90 °C) and, referring to the fluid evolution described by Cochemé *et al.*, (1994), Ca- and K-rich fluids changed their composition as the temperature fell. Depletion of these elements in the fluid during phillipsite formation promoted the appearance of Na-rich zeolites, first revealed by the precipitation of fibrous calc-sodic zeolites (thomsonite), followed by granular calc-sodic analcime and chabazite and Na-rich zeolites as natrolite (similar to that reported by Cochemé *et al.*, 1994). Si activity in the fluid was low during chabazite and analcime crystallisation due to equilibrium with silica phases and more stable phases during this stage. These zeolites must have been formed at lower temperatures; otherwise, if temperature had reached 100 °C, then stable zeolites would have been fibrous, which would have grown at the expense of previously formed zeolites (Chipera and Apps (2001). Hay and Sheppard (2001) have experimentally demonstrated that chabazite is stable up to 100 °C, whereas analcime is stable between 100 and 200 °C. In our case, the textures observed in some amygdales, showing chabazite formation after analcime, would indicate a decrease in temperature. However, according to Chipera and Apps (2001), decreased Si activity reduced the analcime stability field, promoting both natrolite formation after analcime and chabazite and thomsonite replacement by natrolite. Additional reduction of Si in the fluid meant that thomsonite, scolecite and mesolite, along with natrolite/gonnardite, would be the most stable zeolites. This suggested that zeolites formed in the edges of basalt cavities did so at higher temperature and lower Si activity at the beginning of crystallisation, and that lower temperature zeolite species having more aluminous composition would form in the central part of the cavity. Laumontite and stilbite formation can be attributed to the nature of the hydrothermal fluids related to the emplacement of plutons, which were probably more enriched in Ca, Ba, and Sr produced by a late event, taking into account that these zeolites usually appear filling fractures in basalts. Similar laumontite and stilbite association has been reported by Dill *et al.*, (2007) regarding zeolite formation in stockworks.

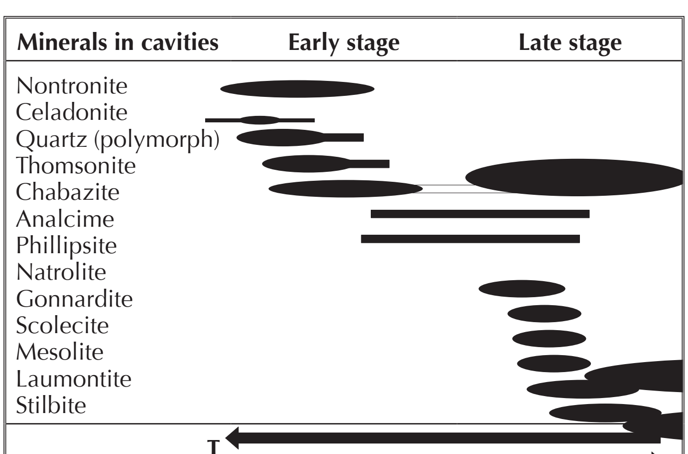

Figure 8. XSequence of mineral phase crystallisation in cavities.

Conclusions

A sequential formation of zeolites and associated secondary minerals filling amygdales and veins in tertiary basaltic host rocks from the Isle of Skye has been described in this study. From early to late formation and, from outermost to innermost portions of the cavities, nontronite, celadonite, thomsonite, phillipsite, chabazite, analcime, natrolite, mesolite, stilbite, scolecite and laumontite and stilbite were sequentially found. However, individual complexly zoned amygdales and veins show evidence of multiple fluid-circulation events, showing a contrast in mineral assemblages from different cavities. Thomsonite, phillipsite, chabazite, analcime, natrolite, mesolite, stilbite and scolecite were associated with nontronite and celadonite in amygdales. Chabazite, analcime, thomsonite, laumontite and stilbite were associated with quartz and calcite in veins. Zeolites deposited in basalts vesicles and veins were the result of a hydrothermal process, having a variety of species and this was due to reduced Si activity in the fluid. Reduced Si activity was also revealed by the absence of SiO_2 polymorphs such as crystoballite, tridymite and opal in the association and because most Na zeolites formed with relatively low Si/Al ratios compared to Ca zeolites. The required amounts of silica, alumina and alkali and alkaline-earth cations necessary for zeolite formation probably resulted from volcanic glass and primary igneous fenocrystal dissolution, although the plagioclase alteration reaction in the rock matrix, releasing Ca, could also have been responsible for this. According to the defined mineral sequence, it can be deduced that a change in fluid composition occurred as temperature dropped. Zeolite formation in the region studied here began with the highest Si activity in fluid and low Si/Al ratio Na zeolites and ended with the lowest Si activity in fluid and high Si/Al ratio Ca zeolites. Secondary minerals nontronite and celadonite represented the first crystallised species lining the outer part of the cavities. Other mineral phases occurring during the early stage were calcite and quartz. Thomsonite was the most common zeolite phase formed after nontronite/celadonite. Na-rich zeolites such as chabazite, analcime, phillipsite and probably wairakite were the first zeolites that became crystallised. They were followed by acicular-fibrous natrolite and Ca-rich zeolites such as gonnardite, thomsonite, mesolite and scolecite. The Si activity decreased during alteration and temperature increased to 200 °C thereby allowing analcime formation followed by that of natrolite, gonnardite, thomsonite, scolecite and mesolite. Laumontite and stilbite formation could be attributed to the presence of Ca, Ba, and Sr-rich hydrothermal fluids produced by a late event, taking into account that these zeolites usually appear filling basalt fractures.

Acknowledgments

We would like to thank the University of Wolverhampton, England, for supporting the research team when carrying out reconnaissance fieldwork on the Isle of Skye, Scotland, during autumn 2008. This research forms part of JM Triana and JF Herrera's Universidad Industrial de Santander undergraduate thesis. We gratefully acknowledge Mrs. Barbara Hodson for assistance with SEM data acquisition at the University of Wolverhampton's School of Applied Sciences and to Mr. Jose Pinto in collecting XRD data at the Universidad Industrial de Santander's Structural Chemistry Laboratory. The authors would also like to thank the anonymous referees for their critical and insightful reading of the manuscript.

References

Alt, J.C, Honnorez, J., Alteration of the upper oceanic crust, DSDP Site 417: mineralogy and chemistry, Contrib. Mineral. Petrol., 87, 1984, pp. 149-169.

Anderson, F.W., Dunham, K.C., The Geology of Northern Skye, Mem. Geol. Surv. U.K., HMSO, Edinburg, 1966, 216p.

Barrer, R.M., Hydrothermal chemistry of zeolites, Academic Press, New York, 1982, 360p.

Bell, B.R., The geochemistry of Lower Tertiary basic dykes the Eastern Red Hills district, Isle of Skye, and their significance for the proposed magmatic evolution of the Skye Centre, Mineral. Mag., 48, 1984, pp. 365-372.

Bell, B.R., Jolley, D.W., Application of palynological data to the chronology of the Palaeogene lava fields of the British Province: implications for magmatic stratigraphy, J. Geol. Soc., 154, 1997, pp. 701-708.

Boles, J., Zeolites in deep-sea sediments. In: F.A. Mumpton (eds.), Mineralogy and Geology of Natural Zeolites Short Course Notes 4, Mineralogical Society of America, Washington, D.C., 1977, pp. 137-163.

Boles, J.R., Coombs, D.S., Zeolite facies alteration of sandstones in the southland syncline, New Zealand, Am. J. Sci., 277, 1977, pp. 982-1012.

Booker, N.A., Cooney, E.L., Priestley, A.J., Ammonia removal from sewage using natural Australian zeolite, Water Sci. Technol., 34, 1996, pp. 17-24.

Breck, D.W., Zeolite Molecular Sieves: Structure, Chemistry and Use, John Wiley, New York, 1974, 313p.

Bustillo, M.A., Martínez-Frías, J., Green opals in hydrothermalized basalts (Tenerife Island, Spain): alteration and aging of silica pseudoglass, J. Non-Cryst. Solids, 323, 2003, pp. 27-33.

Cochemé, J., Aguirre, L., Bevins, R., Robinson, D., Zeolitization processes in basic lavas of the

Baucarit Formation, Northwestern Mexico, Rev. Soc. Geol. Chile, 21, 1994, pp. 217-231.

Deer, W.A., Howie, R.A., Wise, W.S., Zussman, J., An Introduction to Rock-Forming Minerals, Longmans, The Geological Society, London, 2004, 696 p.

Chipera, S., Apps, J., Geochemical stability of natural zeolites. In: D.L. Bish and D.W. Ming (eds.), Natural Zeolites: Occurence, Properties, Applications, Reviews in Mineralogy and Geochemistry, Mineralogical Society of America, 45, Washington, D.C., 2001, pp. 117–161.

Dickin, A.P., Isotope geochemistry of Tertiary rocks from the Isle of Skye, N.W. Scotland, J. Petrol. 21, 1981, pp. 155-189.

Dickin, A.P., Exley, R.A., Isotopic and geochemical evidence for magma mixing in the petrogenesis of the Coire Uaigneich Granophyre, Isle of Skye, NW Scotland, Contrib. Mineral. Petr. 76, 1981, pp. 98–108.

Dill, H.G., Fzssl, M., Botz, R. Mineralogy and (economic) geology of zeolite-carbonate mineralization in basis igneous rocks of the Troodos Complex, Cyprus, Neues Jb. Miner. Abh., 183, 2007, pp. 251-268.

Dixit, L., Prasada, T.S.R., New approach to acid catalysis and hydrocarbon - zeolite interactions, Stud. Surf. Sci. Catal., 113, 1998, pp. 313-319.

Drury, S.A., Frances, P.W., Gass, I.G., Jackson, D.E., Melton, L.R.A., Pearce, J.A., Thorpe, R.S., Williams, D.W., Wilson, R.C.L., Igneous case study. The Tertiary igneous rocks of Skye, NW Scotland, The Open University Press, Milton Keynes, 1976, 115p.

Emeleus, C.H., Gyopari, M.C., British Tertiary Volcanic Province, Geol. Conserv. Rev. Series 4, Chapman and Hall, London, 1992, 259p.

Ferry, J.M., Mutti, L.J., Zuccala, G.J., Contact metamorphism/hydrothermal alteration from the Isle of Skye, northwest Scotland, Contrib. Mineral. Petrol., 95, 1987, pp. 166-181.

Fowler, S.J., Bohrson, W.A., Spera, F.J., Magmatic Evolution of the Skye Igneous Centre, Western Scotland: Modelling of Assimilation, Recharge and Fractional Crystallization, J. Petrol., 45, 2004, pp. 2481–2505.

Garner, P., Continental Flood Basalts Indicate a pre-Mesozoic Flood/post-Flood Boundary, CENTech. J., 10, 1996, pp. 114-127.

Gibbons, W., Harris, A.L., A Revised Correlation of Precambrian Rocks in the British Isles, The Geological Society, Broughton Gifford, 1994, 110p.

Gibson, S.A., The geochemistry of the Trotternish sills, Isle of Skye: crustal contamination in the British Tertiary Volcanic Province, J. Geol Soc. London, 147, 1990, pp. 1071-1081.

Gibson, S.A., Jones, A.P., Igneous stratigraphy and internal structure of the Little Minch Sill Complex, Trotternish Peninsula, northern Skye, Scotland, Geol. Mag., 128, 1991, pp. 51-66.

Giletti, B.J., Moorbath, S., Lambert, R.St.J., A Geochronological Study of the Metamorphic Complexes of the Scottish Highlands, Quart. J. Geol. Soc., 117, 1961, pp. 233-272.

Gillen, C., Geology and landscapes of Scotland, Terra Publishing, Harpenden, 2003, 245p.

Goodenough, K., Bradwell, T., Rum and the Small Isles: A Landscape Fashioned by Geology. Perth, Scotland, Scottish Natural Heritage, 2004, 39p.

Gottardi, G., Galli, E., Natural Zeolites, Springer-Verlag, Berlin, 1985, 409p.

King, P.M., The secondary minerals of the Tertiary lavas of northern and central Skye – zeolite zonation patterns, their origin and formation, Unpublished PhD thesis, University of Aberdeen, 1977.

Hamilton, M.A., Pearson, D.G., Thompson, R.N., Kelley, S.P., Emeleus, C.H., Rapid eruption of Skye lavas inferred from precise U-Pb and Ar-Ar dating of the Rum and Cuillin plutonic complexes, Nature, 394, 1998, pp. 260-262.

Hay, R., Sheppard, R., Occurrence of zeolites in sedimentary rocks: An overview. In: D.L. Bish and D.W. Ming (eds.), Natural Zeolites: Occurence, Properties, Applications, Reviews in Mineralogy and Geochemistry, 45, Washington, D.C., 2001, pp. 217-234.

Keith, T.E., Staples, L.W., Zeolites in Eocene basaltic pillow lavas of the Siletz River Volcanics, central Coast Range, Oregon, Clay Clay Miner. 33, 1985, pp. 135-144.

Kristmannsdóttir, H., Tómasson, J., Zeolites zones in geothermal areas in Iceland. In: L.B. Sand and F.A. Mumpton (eds.), Natural Zeolites: Occurrence, Properties, Use, Pergamon, New York, 1978, pp. 277-284.

Langella, A., Cappelletti, P., de' Gennaro, R., Zeolites in closed hydrologic systems, Rev. Miner. Geochem., 45, 2001, pp. 235-260.

Loiola, A.R., Andrade, J.C.R.A., Sasaki, J.M., da Silva, L.R.D., Structural analysis of zeolite NaA synthesized by a cost-effective hydrothermal method using kaolin and its use as water softener, J. Coll. Int. Sci., 367, 2012, pp. 34-39.

Meier, W.M., Zeolite structures. In: R. Szostak (eds.), Molecular Sieves, Blackie Academic and Professional, London, 1968, pp. 10-27.

Mendum, J.R., Barber, A.J., Butler, R.W.H., Flinn, D., Goodenough, K.M., Krabbendam, M., Park, R.G., Stewart, A.D., Lewisian, Torridonian and Moine Rocks of Scotland, Geological Conservation Review Series, No. 34, Joint Nature Conservation Committee, Peterborough, 2008, 598p.

Ming, D.W., Mumpton, F.A., Zeolites in soils. In: J.B. Dixon and S.B. Weed (eds), Minerals in Soil environments, Soil Science Society of America, Wisconsin, 1989, pp. 873-911.

Misaelides, P., Application of natural zeolites in environmental remediation: A short review, Micropor. Mesopor. Mat., 144, 2011, pp. 15-18.

Moorbath, S., Bell, J.D., Strontium isotope abundance studies and rubidium-strontium age determinations on Tertiary igneous rocks from the Isle of Skye, northwest Scotland, J. Petrol., 6, 1965, pp. 37-66.

Neuhoff, P.S., Fridriksson, T., and Arnórsson, S., Porosity evolution and mineral paragenesis during low-grade metamorphism of basaltic lavas at Teigarhorn, Eastern Iceland, Am. J. Sci., 299, 1999, pp. 467-501.

Orlandi, P., Scortecci, P.B., Minerals of the Elba pegmatites, Mineral. Rec., 16, 1985, pp. 353-364.

Park, R.G., Stewart, A.D., Wright, D.T., The Hebridean terrane. In: N.H. Trewin (eds.), The Geology of Scotland, The Geological Society, London, 2003, pp. 45–61.

Pe-Piper, G., Mode of occurrence, chemical variation and genesis of mordenite and associates zeolites from the Morden Area, Nova Scotia, Canada, Can. Mineral., 38, 2000, pp. 1215-1232.

Saunders, A.D., Fitton, J.G., Kerr, A.C., Norry, M.J., Kent, R.W., The North Atlantic Igneous Province. In: J.J. Mahoney and M.F. Coffin (eds), Large Igneous Provinces: Continental, Oceanic and Planetary Volcanism, Geophysical Monograph, American Geophysical Union, 100, 1997, pp. 45–93.

Seki, Y., Distribution and modes of occurrence of wairakites in the Japanese Island arc, Jour. Geol. Soc. Japan, 79, 1973, pp.521-527.

Surdam, R.C., Low-grade metamorphism of tuffaceous rocks in the Karmutsen Group, Vancouver Island, British Columbia, Geol. Soc. Am. Bull., 84, 1973, pp. 1911-1922.

Strachan, R.A., Smith, M., Harris, A.L., Fettes, D.J., The Northern Highland and Grampian terranes. In: N.H. Trewin (eds.), The Geology of Scotland, The Geological Society, London, 2002, 550p.

Stuart, F.M., Ellam, R.M., Harrop, P.J., Fitton, J.G., Bell, B.R., Constraints on mantle plumes from the helium isotopic composition of basalts from the British Tertiary Igneous Province, Earth Planet. Sc. Lett., 177, 2000, pp. 273-285

Szoztak, R., Molecular sieves, Blackie Academic and Professional, London, 1998, 359p.

Thompson, R.N., Magmatism of the British Tertiary Volcanic Province, Scott. J. Geol., 18, 1982, 49-109.

Townsend, C., Isle of Skye, Collins rambler's guide, HarperCollins Publishers, New York, 2001, 192p.

Trewin, N.H., The Geology of Scotland, The Geological Society of London, 2003, 550p.

Bell, J.D., The Tertiary intrusive complex on the Isle of Skye, Proceedings of the Geologists' Association, 87, 1976, pp. 247-271.

Utada, M., Zeolitic zoning of the Neogene pyroclastic rocks in Japan. Sci. Pap. Coll. Gen. Educ., Univ. Tokyo 21, 1971, pp. 189-221.

Vincent, M.W., Ehlig, P.L., Laumontite mineralization in rocks exposed north of San Andreas Fault at Cajon Pass, southern California, Geophys. Res. Let., 15, 1988, pp. 977-980.

Walker, G.P.L., Zeolite zones and dike distribution in relation to the structure of the basalts of eastern Iceland, J. Geol., 68, 1960, pp. 515-528.

Weisenberger, T., Zeolites in fissures of crystalline basement rocks, Unpublished PhD thesis, Universität Freiburg, 2009.

Weisenberger, T., Selbekk, R.S., Multi-stage zeolite facies mineralization in the Hvalfjördur area, Iceland, Int. J. Earth Sci., 98, 2008, pp. 985-999.

Weisenberger, T., Bucher, K., Zeolites in fissures of granites and gneisses of the Central Alps, J. Metam. Geol., 28, 2010, pp. 825–847.

Weisenberger, T., Spürgin, S., Zeolites in alkaline rocks of the Kaiserstuhl Volcanic Complex, SW Germany - New microprobe investigation and the relationship of zeolite mineralogy to the host rock, Geol. Belgica, 12, 2009, pp. 75-91.

White, R.S., McKenzie, D.P., Magmatism at rift zones: The generation of volcanic continental margins and flood basalts, J. Geophys. Res., 94, 1989, pp. 7685-7729.

Whitehouse, M.J., Bridgwater, D., Geochronological constraints on Paleoproterozoic crustal evolution and regional correlations of the northern Outer Hebridean Lewisian complex, Scotland, Precambrian Res., 105, 2001, pp. 227-245.